Title

Development of Injectable Amniotic Membrane Matrix for Postmyocardial Infarction Tissue Repair.

Journal

Advanced healthcare materials, 9(2)

ISSN

2192-2640

Authors

Henry, Jeffrey JD
Delrosario, Lawrence
Fang, Jun
et al.

Publication Date

2020

DOI

10.1002/adhm.201900544

Peer reviewed

Published in final edited form as:

Adv Healthc Mater. 2020 January ; 9(2): e1900544. doi:10.1002/adhm.201900544.

Development of Injectable Amniotic Membrane Matrix for Post-Myocardial Infarction Tissue Repair

Jeffrey J. D. Henry[#],
Department of Bioengineering, University of California, Berkeley, CA 94720, USA

Lawrence Delrosario[#],
Department of Medicine, Cardiovascular Research Institute and Institute for Regeneration Medicine. University of California, San Francisco, CA 94143, USA

Jun Fang[#],
Department of Bioengineering and Medicine, University of California, Los Angeles, CA 90095

Sze Yue Wong,
Department of Bioengineering, University of California, Berkeley, CA 94720, USA

Qizhi Fang,
Department of Medicine, Cardiovascular Research Institute and Institute for Regeneration Medicine. University of California, San Francisco, CA 94143, USA

Richard Sievers,
Department of Medicine, Cardiovascular Research Institute and Institute for Regeneration Medicine. University of California, San Francisco, CA 94143, USA

Surya Kotha,
Department of Bioengineering, University of California, Berkeley, CA 94720, USA

Aijun Wang,
Department of Surgery, University of California, Davis, CA 95817, USA

Diana Farmer,
Department of Surgery, University of California, Davis, CA 95817, USA

Praneeth Janaswamy,
Department of Medicine, Cardiovascular Research Institute and Institute for Regeneration Medicine. University of California, San Francisco, CA 94143, USA

Randall J. Lee,
Department of Medicine, Cardiovascular Research Institute and Institute for Regeneration Medicine. University of California, San Francisco, CA 94143, USA

Song Li
Department of Bioengineering, University of California, Berkeley, CA 94720, USA

Department of Bioengineering and Medicine, University of California, Los Angeles, CA 90095

songli@ucla.edu.
[#]Drs. Henry, Delrosario and Fang contributed equally to this work.

Abstract

Ischaemic heart disease represents the leading cause of death worldwide. Heart failure following myocardial infarction (MI) is associated with severe fibrosis formation and cardiac remodeling. Recently, injectable hydrogels have emerged as a promising approach to repair the infarcted heart and improve heart function through minimally invasive administration. Here, we developed a novel injectable human amniotic membrane (hAM) matrix to enhance cardiac regeneration following MI. Human amniotic membrane was isolated from human placenta and engineered to be a thermo-responsive, injectable gel around body temperature. Ultrasound-guided injection of hAM matrix into the rat MI hearts significantly improved cardiac contractility, as measured by ejection fraction (EF), and decreased fibrosis. Our results demonstrate the feasibility of engineering an injectable hAM matrix and its efficacy in attenuating degenerative changes in cardiac function following MI, which may have broad applications in tissue regeneration.

Graphical Abstract

Keywords

myocardial infarction; amniotic membrane; hydrogel; decellularization

1. Introduction

Myocardial infarction (MI) associated heart failure is the leading cause of death in the U.S.[1] MI occurs when blood flow to the heart from coronary arteries is occluded, causing ischemia and subsequent myocardial tissue death. Myocardial tissue is unable to effectively regenerate following MI, thus leading to scar formation, left ventricular remodeling, and eventual heart failure.[2,3] Several tissue engineering strategies have been developed to prevent scarring and promote cardiac regeneration, including cell-based therapies, porous scaffolds, cardiac patches and hydrogels.[4–9] Among them, an injectable natural or synthetic hydrogel is minimally invasive and promising for in situ cardiac tissue repair for infarcted hearts.[10]

Decellularized mammalian Extracellular matrix (ECM), as a natural material, has been extensively investigated in regenerative medicine.[11–18] ECM hydrogel retains the full biochemical complexity and inherent bioactivity of the native matrix, which could facilitate tissue regenerative capability.[8,19,20] Although certain properties of ECM hydrogels are widely conserved regardless of source tissue, some characteristics vary markedly and are influenced by source species, source tissue and processing methods. In particular, human amniotic membrane (hAM) can be easily obtained and processed from the placenta without ethical concerns. The matrix derived from human amniotic membrane has various

components and bioactivities, which allow such matrix to be widely applied in corneal transplantation, retinal regeneration, liver regeneration, and wound healing.[21–24] Due to its anti-inflammatory effects, anti-fibrotic effect, and angiogenic potentials,[25–28] we postulate that materials derived from hAM could beneficial for restoring cardiac function following MI.

Here we report a method to decellularize hAM matrix. The remaining contents of DNA, glycosaminoglycan and collagen are measured. In vitro cell culture shows cell proliferation and biological activities of hAM matrix are preserved. Additionally, the thermos-responsive hAM matrix hydrogel can be injected into the rat MI hearts and demonstrates beneficial effects to enhance cardiac ejection fraction and reduce fibrosis.

2. Methods

2.1 Decellularization of Human Amniotic Membrane (hAM)

Full term human placentas with intact hAM were obtained from healthy donors undergoing caesarean section at the University of California, San Francisco or University of California, Davis Hospitals. The hAM was then identified and separated from the placenta and weighed. The tissue was subsequently frozen at −80°C for 48 hours and thawed prior to decellularization. The membrane was thoroughly rinsed with water and soaked in 1 N NaCl for 15 minutes. Membranes were then treated in a solution containing 8 mM CHAPS (3-((3-cholamidopropyl) dimethylammonio)-1-propanesulfonate), 25 mM EDTA, and 1M NaCl at room temperature with moderate agitation. The CHAPS solution was removed and replenished every 2 hours, for 6 hours total. For comparison purposes, 8 mM SDS (sodium dodecyl sulfate) was used instead of CHAPS. Following CHAPS or SDS treatment, all membranes were subsequently washed with Tris-buffered saline (TBS, 3 times, 20 minutes each). To remove remaining nucleic acid material, membranes were incubated in a 90 U/ml benzonase solution (Sigma Aldrich Inc., St. Louis, MO) for 15 hours at 37°C. To enhance nuclease activity, benzonase was prepared in 50mM Tris-HCL pH 8.0, with 0.1 mg/ml BSA, and 1mM $MgCl_2$. Following benzonase treatment, hAMs were washed repeatedly in TBS, followed by repeated washes with distilled water. hAMs were further decellularized and disinfected using a 0.1% peracetic acid,4% ethanol and water. After repeated washing in TBS, and distilled water, hAMs were dialyzed against water at 4°C for 4 days to remove excess reagents.

Following dialysis, portions of the decellularized hAM were snap-frozen in OCT compound (Sakura Finetek, Torrance, CA) and sectioned for histological analysis. Intact and untreated hAM was also frozen and sectioned for comparison. Sections were stained with DAPI or Hematoxylin & Eosin to visualize nuclei and matrix components respectively.

2.2 Preparation of Injectable hAM Matrix

Decellularized hAMs were lyophilized overnight and subsequently ground into a dry powder using a motorized grinder. The decellularized hAM powder was solubilized by digestion in 0.2 mg/ml pepsin and 0.1N HCL for 48 hours at room temperature. A ratio of 20 mg hAM matrix per 1ml pepsin/HCL solution was used. After 48 hours, the solution pH was adjusted

to 8.0 using 10N NaOH and 10x PBS. The pH adjusted matrix was then re-lyophilized overnight, ground into powder form, and stored at 4°C. Prior to experiments, the hAM matrix was sterilized in ethylene oxide gas overnight. To induce gelation, hAM matrix was dissolved in PBS (20 mg/ml) and allowed to gel at 37°C.

2.3 Characterization of Injectable hAM Matrix

The remaining DNA content in the injectable hAM matrix was quantified using a Quant-iT™ PicoGreen® Assay (Invitrogen, Grand Island, NY). A DNeasy Blood & Tissue Kit® (Qiagen, Valencia, CA) was used to isolate DNA prior to quantification using the assay. The DNA content of CHAPS processed hAM matrix, and SDS processed hAM matrix is presented as a percentage of native, untreated hAM tissue.

Glycosaminoglycans (GAGs) are often reported to be lost following decellularization of tissue. For this reason, we quantified the GAG content of both CHAPS processed hAM matrix and SDS processed hAM matrix. GAG content was quantified using a colorimetric 1,9 dimethylmethylene blue (DMMB) assay as described previously.[29] This reagent specifically binds to the sulfate and carboxyl groups of sulfated GAGs to cause a metachromatic shift. This shift in absorption can then be quantified via spectroscopy at 530 nm. Lyophilized powder native and decellularized hAM tissue was first digested using proteinase K (1mg proteinase K/80mg hAM matrix). DMMB reagent (16μg/mL) was then allowed to react with the samples. GAG content in each sample was then immediately quantified by measuring the absorbance at 530nm and comparing to values obtained using known GAG concentrations. Final GAG content is given as a percentage of GAG content in the native tissue. The hAM matrix processed using CHAPS contained the highest amount of preserved GAG content. For this reason, the CHAPS hAM matrix was used in all *in vitro* and *in vivo* experiments.

The collagen content of the decellularized hAM matrix was measured by a hydroxyproline assay kit (Cell Biolabs Inc) by following the vendor's protocol as previously described.[30] Briefly, hAM powder was hydrolyzed by 12N hydrochloric acid for 3 hours at 120ºC to free hydroxyproline. The acid-hydrolyzed samples were further dried under vacuum evaporation at 80ºC for 40 minutes. Then chloramine T mixture was added to convert the hydroxyproline to a pyrrole. Finally, Ehrlichs Reagent was added to the solution to react with the pyrrole and produce a chromophore. The absorbance of the samples was measured at 540 nm and quantified by a standard curve of hydroxyproline. The collagen content was calculated by using the estimation that hydroxyproline makes up 13.5% of collagen.

Mass spectrometry was performed in order to survey the overall protein composition of the injectable hAM matrix. Samples were digested with trypsin and desalted with C18 spec tips prior to analysis. Proteins were separated and analyzed at the Vincent J. Coates Proteomics/Mass Spectrometry Laboratory by using multidimensional protein identification technology (MudPIT) with two-dimensional HPLC separation-tandem mass spectrometry. Peptide identification and data analysis were performed using SEQUEST.

2.4 Mechanical Characterization of Injectable hAM Matrix

Oscillatory rheology analysis was performed on a MCR 301 rheometer (Anton Paar). hAM matrix (400 μl) was allowed to gel for 1 hr at 37°C on the rheometer between parallel plates with a 25-mm top probe at 0.81mm gap width in a humidified chamber. Frequency sweep was performed from 10–0.1 Hz at 1% strain amplitude. Shear modulus was reported as the average of 5 storage modulus measurements taken at 1 Hz.

2.5 *In vitro* Characterization of Cell Growth on Injectable hAM Matrix

In vitro biocompatibility was examined by investigating the effect of injectable hAM matrix on the proliferation of bovine arterial endothelial cells (BAECs). BAECs were harvested from fresh bovine aortas as previously described using collagenase and gentle scrapping with a policeman.[31] All cells were cultured in Dulbecco's Modified Eagle Medium (DMEM) supplemented with 10% fetal bovine serum (FBS) and 1% penicillin/streptomycin antibiotic mix. Cell culture was maintained in a humidified incubator at 37 °C.

For proliferation experiments, the surfaces of a 24-well tissue culture plate were coated with either 1 mg/ml rat tail collagen type-1 (BD Biosciences) or 5 mg/ml injectable hAM matrix. BAEC were seeded on coated surfaces at low density (1000 cells/cm^2), medium density (5,000 cells/cm^2), and high density (10,000 cells/cm^2). After 48 hours, BAEC proliferation on hAM matrix and collagen type-1 surfaces was then measured and compared using a Click-iT® EdU Alexa Fluor® 488 Detection Kit (Life Technologies Inc). Samples were counterstained using DAPI. Cell proliferation is given as the percent of EdU positive cells.

In addition, cell biocompatibility and viability were evaluated. Live/dead staining (Live/Dead staining Kit, Thermo Fisher Scientific) was employed to show the cell biocompatibility on either hAM matrix or collagen-I at days 2 and 6. ECs were seeded at 5000 cells/cm^2. Fluorescent images were taken using Zeiss Axio Observer Z1 inverted microscope to visualize stained cells. Furthermore, the cell viability was quantitatively measured by PrestoBlue® assay (Thermo Fisher Scientific).

2.6 Myocardial Infarction (MI) Model

All surgical procedures were approved by the Committee for Animal Research of the University of California, San Francisco. The ischemia-reperfusion model used in this study has been previously used extensively as a model for MI.[32,33] Female Sprague-Dawley rats (225–250 g) were anesthetized with ketamine (90 mg/kg) and xylazine (10 mg/kg). The chest was opened by a median sternotomy, and a single stitch of 7–0 Ticron suture (Tyco Healthcare, Norwalk, CT) was introduced around the left anterior descending (LAD) coronary artery and tightened to occlude for 30 min before reperfusion and closing the thoracic cavity. The animals were allowed to recover for 2 days after ischemia-reperfusion prior to treatment.

2.7 *In vivo* hAM Matrix Injection Studies

At 2 days post-MI, rats in the study group were randomized into hAM matrix (n = 5) or PBS control groups (n = 5). The animals were anesthetized using 2% isoflurane at 2 liters/minute and positioned on the echo-guided ultrasound apparatus. Echocardiography was performed

prior to injection. Echocardiography directed intramyocardial injection of either 500 μL of sterile phosphate buffered saline (PBS) (UCSF Cell Culture Facility, San Francisco, CA) containing no hAM or 10 mg of hAM using a 27-gauge needle was delivered to the superior pole, center, and inferior pole of the infarct region as visualized by hyper-echoicity on ultrasound as previously described (Vevo 660, Visual Sonics, Toronto, Canada).[34] The successful injection was confirmed visually by changes in ultrasound signal in the vicinity of the syringe.

2.8 Functional Recovery of LV function after hAM Matrix Injection

Transthoracic echocardiography was performed immediately prior to injection, and 5 weeks after injection. Echocardiograms were used to calculate ejection fraction and fractional shortening before and after treatment. Ejection fraction was calculated as described previously.[35] A parasternal long-axis B-mode image was acquired in order to identify the maximum LV length. Three short-axis B-mode images were also acquired at basal, midventricular, and apical LV levels. Results are presented as the percent change in ejection fraction and percent change in fractional shortening. Using frames from the long axis images, as well as maximum and minimum cross-sectional areas in the heart cycle, LV end-systolic volume (LVESV) and LV end-diastolic volume were calculated. LV Ejection Fraction (LVEF) was calculated as follows, LVEF = ((LVEDV – LVESV)/LVEDV) x 100. Results are given as the percent change in LVEF 5 weeks post-injection. Left ventricular inner dimensions at systole (LVIDs) and diastole (LVIDd) were calculated using the leading edge method, as prescribed by the American Society of Echocardiography. Fractional shortening, FS was calculated as follows, ((LVIDd – LVIDs)/LVIDd) x 100. Results are presented as the percent change in FS 5 weeks post-injection

2.9 Histology

Five weeks post-treatment, the rats perfused with 3M KCl prior to sacrifice to arrest the hearts in the diastolic phase. The hearts were harvested, rinsed in cold saline, blotted-dry and fresh frozen in Tissue Tek O.C.T. freezing medium (Sakura Finetek, Torrance, CA). The hearts were sectioned into 10 μm slices. Sequential slides spanning the LV region were stained with Masson's-trichrome stain and were used for morphological assessment of the infarct size as previously described.[36] Briefly, Masson's-trichrome staining images were used to evaluate the infarct size with Image J software. The infarct size (% LV) was calculated by dividing the collagen deposited area to the entire left ventricle area near the midsection of the infarct area. Three sections for each sample were measured.

2.10 Statistics

All experiments are performed in triplicate unless otherwise mentioned. *In vitro* and *in vivo* data are presented as mean ± standard deviation. All data were compared with one-way ANOVA tests. Holm's t-test was performed to evaluate significant differences between pairs. A p-value of less than 0.05 was considered statistically significant.

3. Results

3.1 Characterization of injectable human amniotic membrane (hAM) matrix

An injectable hAM matrix was prepared through decellularization of hAM tissue (Fig. 1A&B). Using a series of chemical treatments, which included the use of either CHAPS or SDS detergent, hAM tissue was successfully decellularized, and lyophilized into power (Fig. 1C). The solubilized hAM matrix remained a viscous liquid while on ice or at room temperature. Gelation could be induced when placed at 37 °C, as the resulting material became a soft gel that required gentle handling (Fig 1D). The hAM gel had a shear modulus of 7.5 ± 2.4 Pa as determined by oscillatory rheometry.

The decellularized tissue was sectioned and stained for nuclei using either DAPI or hematoxylin & eosin (H&E) stain. Both CHAPS and SDS decellularization processes were successful, as both tissues groups appeared devoid of cells (Fig. 2). The general matrix structure of native, CHAPS decellularized and SDS decellularized hAM was visualized using H&E staining (Fig. 2 A–C). The matrix structure of CHAPS decellularized hAM appears to be minimally altered in comparison to native hAM. In contrast, the matrix structure of SDS decellularized hAM appears significantly altered when compared to the structure of native hAM. DAPI staining (Fig. 2 D–F) showed that cell nuclei were removed by either CHAPS or SDS treatment.

In order to quantify the efficiency of decellularization protocols, remaining DNA content within the decellularized hAM matrix was quantified (Fig. 2G). The amount of DNA/mg of both SDS and CHAPS processed tissue was measured as a percentage of the amount of DNA/mg of untreated hAM tissue. Following CHAPS and SDS decellularization, little DNA content was detected. GAGs are a critical component of the extracellular matrix and also are a component commonly lost after decellularization. For this reason, the GAG content within CHAPS and SDS decellularized hAM was measured (Fig. 2H). GAG content was measured as a percentage of the GAG content found within native, untreated hAM. After CHAPS decellularization, GAGs were relatively conserved, as 85.6% of the native GAG in hAM was retained. In contrast, however, only 10.1% of native GAG content was retained following decellularization using SDS. In addition, collagens are most abundant matrix proteins in the animal or human tissues. We found that more than 45% collagens were retained after the CHAPS decellularization process, which was slightly higher than SDS decellularization method (~41%). Since effective decellularization could be achieved using CHAPS with higher GAG/matrix components and collagen content, CHAPS-processed hAM was used in further *in vitro* and *in vivo* experiments.

The composition of the injectable hAM matrix was characterized by the mass spectrometry analysis (Table S1). This identified and confirmed some major matrix components, including different types of collagen, fibronectin, laminin, keratin, fibrillin and growth factor receptors.

3.2 *In vitro* studies using bovine aortic endothelial cells (BAECs)

To assess the biocompatibility of the injectable hAM matrix, the proliferation of BAECs on hAM matrix was measured. As a positive control of biocompatibility, the proliferation of

BAECs on type-1 collagen was also measured. At low density (1000 cells/cm^2), medium density (5,000 cells/cm^2), and high density (10,000 cells/cm^2), there was no significant difference in proliferation on hAM matrix-coated surfaces, when compared to proliferation on Collagen-1 surfaces with similar cell densities (Fig. 3 A&B).

In addition, the cell biocompatibility of hAM matrix-coated surface was measured by live/dead cell staining at days 2 and 6 (Figure 3C). The majority of ECs were alive during the cell culture period and became confluent after 6 days on hAM matrix. In support of this visual trend, the cell viability was measured by PrestoBlue® assay (Figure 3D). Compared to commonly used collagen, no significant differences in proliferation, biocompatibility and viability were observed, suggesting that decellularized hAM matrix had excellent biocompatibility and biological activities for cell growth.

3.4 Recovery of LV function following hAM Matrix Injection

In vivo studies were performed by injecting hAM matrix into the acute infarcted myocardium. After 5 weeks following injection, hAM matrix-treated group showed significantly higher LVEF than PBS-treated group (57±7.1 % for hAM vs 34±3.5 % for PBS) (Fig. 4 A). Compared to the pre-treatment time point (Day 2 post-MI), the PBS-treated group generally demonstrated a continued decline in LV function (−9.7% worsening), while hAM matrix treatment prevented the negative LV remodeling and showed a significant improvement of LV function (+8.8%) (Fig. 4 B&C).

Fractional shortening also improved for animals receiving hAM matrix following acute MI (Fig. 4D). Improvements in fractional shortening were observed in all animals treated with hAM matrix injection. A decline in fractional shortening following acute MI was observed for all animals receiving PBS injection. On average, animals receiving hAM matrix injection experienced a +10.5% increase in fractional shortening, while animals receiving PBS injection experienced a −12.4% decline in fractional shortening.

3.5 MI size.

After 5 weeks, the MI rat hearts were harvested and cryosectioned for histological analyses. The cardiac fibrosis for hAM matrix or PBS treated hearts was evaluated with Masson's trichrome staining. Consistent with the functional analysis, there was a significant decrease in MI size as a percentage of the total LV in the hAM matrix treated group compared to the PBS group (Fig. 5). Infarct size was significantly reduced in the hAM matrix treated rats compared to the PBS treated rats ($p < 0.05$).

4. Discussion

Heart failure following MI is a progressive process, consisting of several stages. During the acute phase, cardiomyocyte death occurs and is followed by macrophage, monocyte and neutrophil migration. The inflammatory response continues through the subacute phase, until cellular components begin to be replaced by dense collagen fibrils. During the chronic phase, infarct expansion occurs, leading to dilation and continued LV remodeling.[37,38] The injectable hydrogel, as a scaffold-based method, has shown great potential to treat MI by providing mechanical support and increasing myocardial thickness to prevent negative

ventricular remodeling, which is advantageous as a minimally invasive and localized treatment[10]. For example, the use of alginate-based hydrogel, Algisyl-LVR, has shown encouraging preclinical results to improve myocardial functionality.[39,40] The goal of this study was to develop an injectable ECM derived from human amniotic tissue and investigate its potential to promote recovery following myocardial infarction. To date, this study is the first to report the development of an injectable scaffold derived from decellularized amniotic membrane. Previous studies have utilized decellularization methods to fabricate injectable scaffolds from urinary bladder matrix, myocardial matrix, and lipoaspirate matrix.[41] Our hypothesis is that hAM matrix may promote scarless wound healing similar to other fetal tissue, which allows regenerative remodeling. It is possible that some scar-inducing components in missing in hAM matrix or hAM matrix has anti-scar molecules, which needs further investigation.

The composition of ECM is unique to the organ/tissue from which it is derived. Likewise, decellularization methods must be tailored and made unique according to the tissue of interest. Through experimentation of various decellularization techniques, we have identified a process that is capable of preserving extracellular components, most specifically, the natural GAGs, from amniotic membrane. This process is highly efficient in removing cellular contents, as seen in the removal of greater than 96% of native DNA content. For future studies, it will be helpful to determine if higher levels of decellularization are needed to yield non-immunogenic matrix products. Additionally, it is valuable to identify and quantify the protein components of the decellularized matrix by more advanced mass spectrum analysis to understand the material properties and biological effects.[42,43]

Through *in vitro* cell studies on bovine aortic endothelium, we found that the injectable hAM matrix was non-cytotoxic, and did not affect cell proliferation. In the future, it will be helpful to determine the effects on cell proliferation, attachment, and migration for other cardiac-specific cell lines. In addition, it will be helpful to determine if the extracted hAM matrix is capable of affecting myofibroblast differentiation, an event central to the process of scar formation.

To investigate the effect of hAM matrix injection on functional LV recovery following myocardial infarction, an acute rodent rat MI model was applied. We found that hAM matrix injection contributed to a reduction in MI scar formation and an improvement in LV function. Significant LV ejection fraction improvement was seen when each animal was used as its own control and with the hAM matrix group was compared to the control group. Due to the diversity in physiological response across various stages after MI, we chose to examine the effects of hAM matrix injection on cardiac function during the acute MI, 2 days after an MI. Hydrogel injection at 2–3 days post-MI has been commonly performed for acute MI therapy as a model to demonstrate therapeutic effects.[36,44] In the future, it will be valuable to evaluate the therapeutic effects of hAM matrix in chronic MI models, which will facilitate the translation of this technology into clinical applications.

Future studies will need to elucidate the potential mechanism of LV functional improvement from hAM matrix injection will require a comparison to the effects of other matrix materials. By adding additional matrix groups to the study, it can be confirmed whether LV

functional improvement from hAM matrix injection is due to the unique biochemical environment of the amniotic membrane, or if LV improvement is due to a mechanical constrainment of LV dilation. To further elucidate the mechanism of action, additional *in vitro* studies should be performed which analyze the effects on myofibroblasts, and other cardiac-specific stem cell populations. Furthermore, before entering clinical trials, large animal models are required for this hAM matrix-based MI therapy.

Supplementary Material

Refer to Web version on PubMed Central for supplementary material.

Acknowledgement

This work was supported in part by grants from the National Institute of Health (HL117213, HL121450 to S.Li and predoctoral fellowship HL094162–04), the Ford Foundation (JH) and the Siebel Scholars Foundation (JH).

References

[1]. Cahill TJ, Choudhury RP, Riley PR, Nat. Rev. Drug Discov 2017, 16, 699. [PubMed: 28729726]

[2]. Kim GH, Uriel N, Burkhoff D, Nat. Rev. Cardiol 2018, 15, 83. [PubMed: 28933783]

[3]. Tallquist MD, Molkentin JD, Nat. Rev. Cardiol 2017, 14, 484. [PubMed: 28436487]

[4]. Hashimoto H, Olson EN, Bassel-Duby R, Nat. Rev. Cardiol 2018, 15, 585. [PubMed: 29872165]

[5]. Parsa H, Ronaldson K, Vunjak-Novakovic G, Adv. Drug Deliver. Rev 2016, 96, 195.

[6]. Mahmoudi M, Yu M, Serpooshan V, Wu JC, Langer R, Lee RT, Karp JM, Farokhzad OC, Nat. Nanotechnol 2017, 12, 845. [PubMed: 28875984]

[7]. Gourdie RG, Dimmeler S, Kohl P, Nat. Rev. Drug Discov 2016, 15, 620. [PubMed: 27339799]

[8]. Chen WCW, Wang ZG, Missinato MA, Park DW, Long DW, Liu HJ, Zeng XM, Yates NA, Kim K, Wang YD, Sci. Adv 2016, 2.

[9]. Becker M, Maring JA, Schneider M, Herrera Martin AX, Seifert M, Klein O, Braun T, Falk V, Stamm C, Int. J. Mol. Sci 2018, 19.

[10]. Hasan A, Khattab A, Islam MA, Abou Hweij K, Zeitouny J, Waters R, Sayegh M, Hossain MM, Paul A, Adv. Sci 2015, 2.

[11]. Bejleri D, Davis ME, Adv. Healthc. Mater 2019, 8, 1801217.

[12]. Jin Y, Lee JS, Kim J, Min S, Wi S, Yu JH, Chang GE, Cho AN, Choi Y, Ahns DH, Cho SR, Cheong E, Kim YG, Kim HP, Kim Y, Kim DS, Kim HW, Quan Z, Kang HC, Cho SW, Nat. Biomed. Eng 2018, 2, 522. [PubMed: 30948831]

[13]. Taylor DA, Sampaio LC, Ferdous Z, Gobin AS, Taite LJ, Acta Biomater. 2018, 74, 74. [PubMed: 29702289]

[14]. Yu C, Ma X, Zhu W, Wang P, Miller KL, Stupin J, Koroleva-Maharajh A, Hairabedian A, Chen S, Biomaterials 2019, 194, 1. [PubMed: 30562651]

[15]. Ma XY, Yu C, Wang PR, Xu WZ, Wan XY, Lai CSE, Liu J, Koroleva-Maharajh A, Chen SC, Biomaterials 2018, 185, 310. [PubMed: 30265900]

[16]. Ghuman H, Mauney C, Donnelly J, Massensini AR, Badylak SF, Modo M, Acta Biomater. 2018, 80, 66. [PubMed: 30232030]

[17]. Zhu Y, Hideyoshi S, Jiang HB, Matsumura Y, Dziki JL, LoPresti ST, Huleihel L, Faria GNF, Fuhrman LC, Lodono R, Badylak SF, Wagner WR, Acta Biomater. 2018, 73, 112. [PubMed: 29649634]

[18]. Hussey GS, Keane TJ, Badylak SF, Nat. Rev. Gastro. Hepat 2017, 14, 540.

[19]. Moroni F, Mirabella T, Am. J. Stem Cells 2014, 3, 1. [PubMed: 24660110]

[20]. Saldin LT, Cramer MC, Velankar SS, White LJ, Badylak SF, Acta. Biomater 2017, 49, 1. [PubMed: 27915024]

[21]. Hariya T, Tanaka Y, Yokokura S, Nakazawa T, Biomaterials 2016, 101, 76. [PubMed: 27267629]

[22]. Ben M'Barek K, Habeler W, Plancheron A, Jarraya M, Regent F, Terray A, Yang Y, Chatrousse L, Domingues S, Masson Y, Sahel JA, Peschanski M, Goureau O, Monville C, Sci. Transl. Med 2017, 9.

[23]. Despeyroux A, Duret C, Gondeau C, Perez-Gracia E, Chuttoo L, de Boussac H, Briolotti P, Bony C, Noel D, Jorgensen C, Larrey D, Daujat-Chavanieu M, Herrero A, J. Tissue Eng. Regen. M 2018, 12, 1062. [PubMed: 29106037]

[24]. Stern M J Amer. Med. Assoc 1913, 60, 973.

[25]. Shimmura S, Shimazaki J, Ohashi Y, Tsubota K, Cornea 2001, 20, 408. [PubMed: 11333331]

[26]. Hashim SNM, Yusof MFH, Zahari W, Noordin KBAA, Kannan TP, Hamid SSA, Mokhtar KI, Ahmad A, Tissue Eng. Regen. Med 2016, 13, 211. [PubMed: 30603401]

[27]. Navas A, Magana-Guerrero FS, Dominguez-Lopez A, Chavez-Garcia C, Partido G, Graue-Hernandez EO, Sanchez-Garcia FJ, Garfias Y, Stem Cell Transl. Med 2018, 7, 906.

[28]. Niknejad H, Peirovi H, Jorjani M, Ahmadiani A, Ghanavi J, Seifalian AM, Eur. Cells Mater 2008, 15, 88.

[29]. Farndale RW, Buttle DJ, Barrett AJ, Biochim. Biophys. Acta 1986, 883, 173. [PubMed: 3091074]

[30]. Lee JY, Kim H, Ha DH, Shin JC, Kim A, Ko HS, Cho DW, Adv. Healthc. Mater 2018, 7, e1800673.

[31]. Li S, Kim M, Hu YL, Jalali S, Schlaepfer DD, Hunter T, Chien S, Shyy JY, J. Biol. Chem 1997, 272, 30455.

[32]. Christman KL, Fok HH, Sievers RE, Fang Q, Lee RJ, Tissue Eng. Part B-Re 2004, 10, 403.

[33]. Huang NF, Sievers RE, Park JS, Fang Q, Li S, Lee RJ, Nat. Protoc 2006, 1, 1596. [PubMed: 17406452]

[34]. Mihardja SS, Gonzales JA, Gao D, Sievers RE, Fang Q, Stillson CA, Yu J, Peng M, Lee RJ, Biomaterials 2013, 34, 8869. [PubMed: 23895998]

[35]. Yu JS, Christman KL, Chin E, Sievers RE, Saeed M, Lee RJ, J. Thorac. Cardiov. Sur 2009, 137, 180.

[36]. Le LV, Mohindra P, Fang QZ, Sievers RE, Mkrtschjan MA, Solis C, Safranek CW, Russell B, Lee RJ, Desai TA, Biomaterials 2018, 169, 11. [PubMed: 29631164]

[37]. Anderson JL, Morrow DA, N. Engl. J. Med 2017, 376, 2053. [PubMed: 28538121]

[38]. Hausenloy DJ, Yellon DM, Nat. Rev. Cardiol 2011, 8, 619. [PubMed: 21691310]

[39]. Lee LC, Wall ST, Klepach D, Ge L, Zhang ZH, Lee RJ, Hinson A, Gorman JH, Gorman RC, Guccione JM, Int. J. Cardiol 2013, 168, 2022. [PubMed: 23394895]

[40]. Lee RJ, Hinson A, Bauernschmitt R, Matschke K, Fang Q, Mann DL, Dowling R, Schiller N, Sabbah HN, Int. J. Cardiol 2015, 199, 18. [PubMed: 26173169]

[41]. Johnson TD, Braden RL, Christman KL, Methods Mol. Biol 2014, 1181, 109. [PubMed: 25070331]

[42]. Zhang X, Fang A, Riley CP, Wang M, Regnier FE, Buck C, Anal. Chim. Acta 2010, 664, 101. [PubMed: 20363391]

[43]. Johnson TD, Hill RC, Dzieciatkowska M, Nigam V, Behfar A, Christman KL, Hansen KC, Proteomics Clin. Appl 2016, 10, 75. [PubMed: 26172914]

[44]. Yoshizumi T, Zhu Y, Jiang H, D'Amore A, Sakaguchi H, Tchao J, Tobita K, Wagner WR, Biomaterials 2016, 83, 182. [PubMed: 26774561]

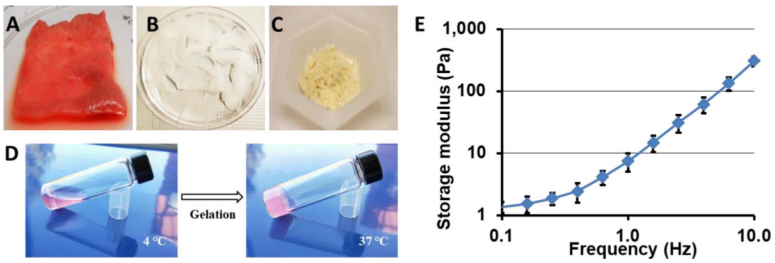

Figure 1. Physical appearance of hAM matrix during various stage of processing.

(A) Untreated hAM prior to decellularization. **(B)** Decellularized hAM tissue. **(C)** Lyophilized and ground soluble hAM matrix. **(D)** Gelation of decellularized hAM matrix at 37 °C. **(E)** Rheological measurement for storage modulus of hAM matrix between oscillatory frequencies 10 and 0.1 Hz at 1% strain amplitude. Data presented as a mean of 5 separate measurements ± one standard deviation.

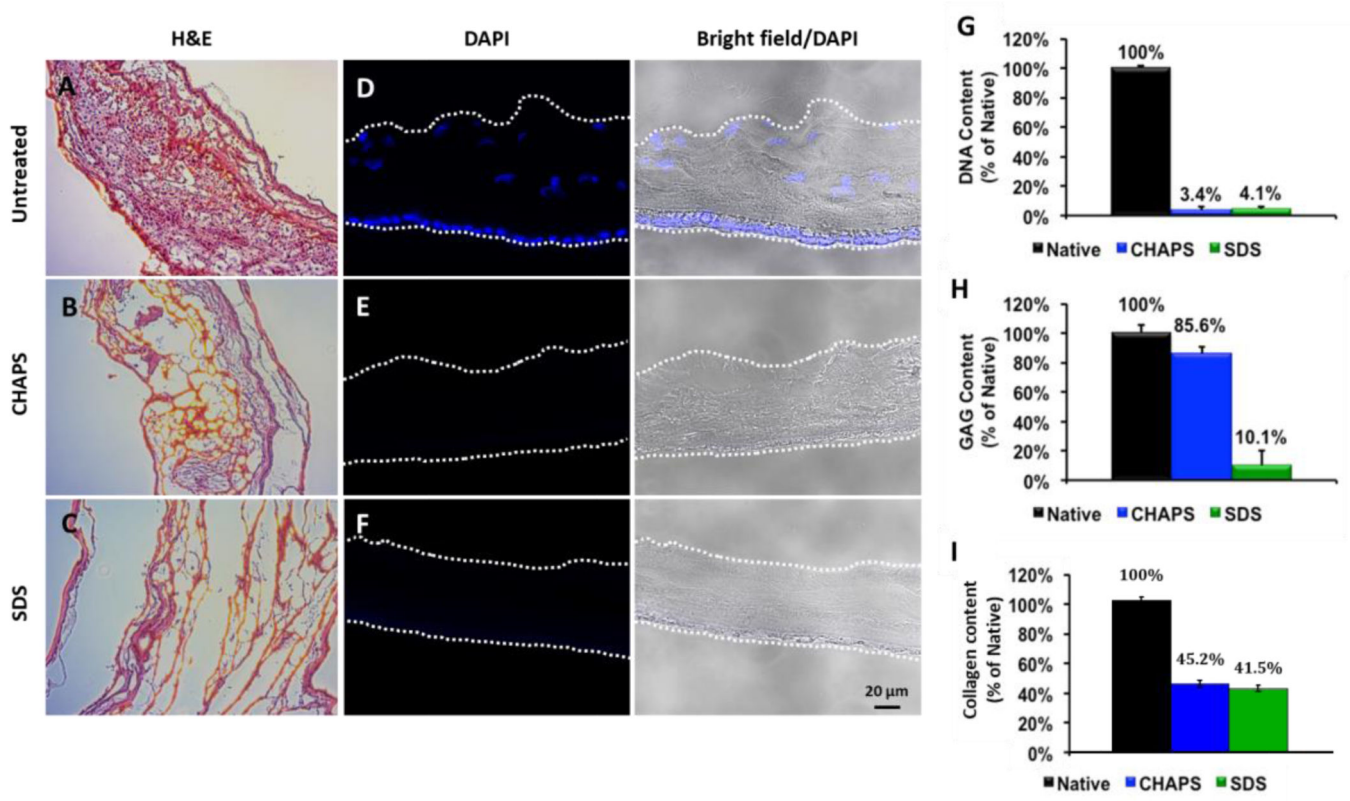

Figure 2. Histological and biochemical characterization of CHAPS and SDS decellularized hAM tissue.

(A-C) Representative H&E staining images of untreated, CHAPS decellularized and SDS decellularized hAM. **(D-F)** DAPI staining of nuclei present in untreated, CHAPS decellularized, and SDS decellularized hAM. **(G)** Percentage of DNA content remaining after CHAPS or SDS decellularization. (H) Percentage of glycosoaminoglycan (GAG) content remaining after CHAPS or SDS decellularization. **(I)** Percentage of collagen content remaining after CHAPS or SDS decellularization.

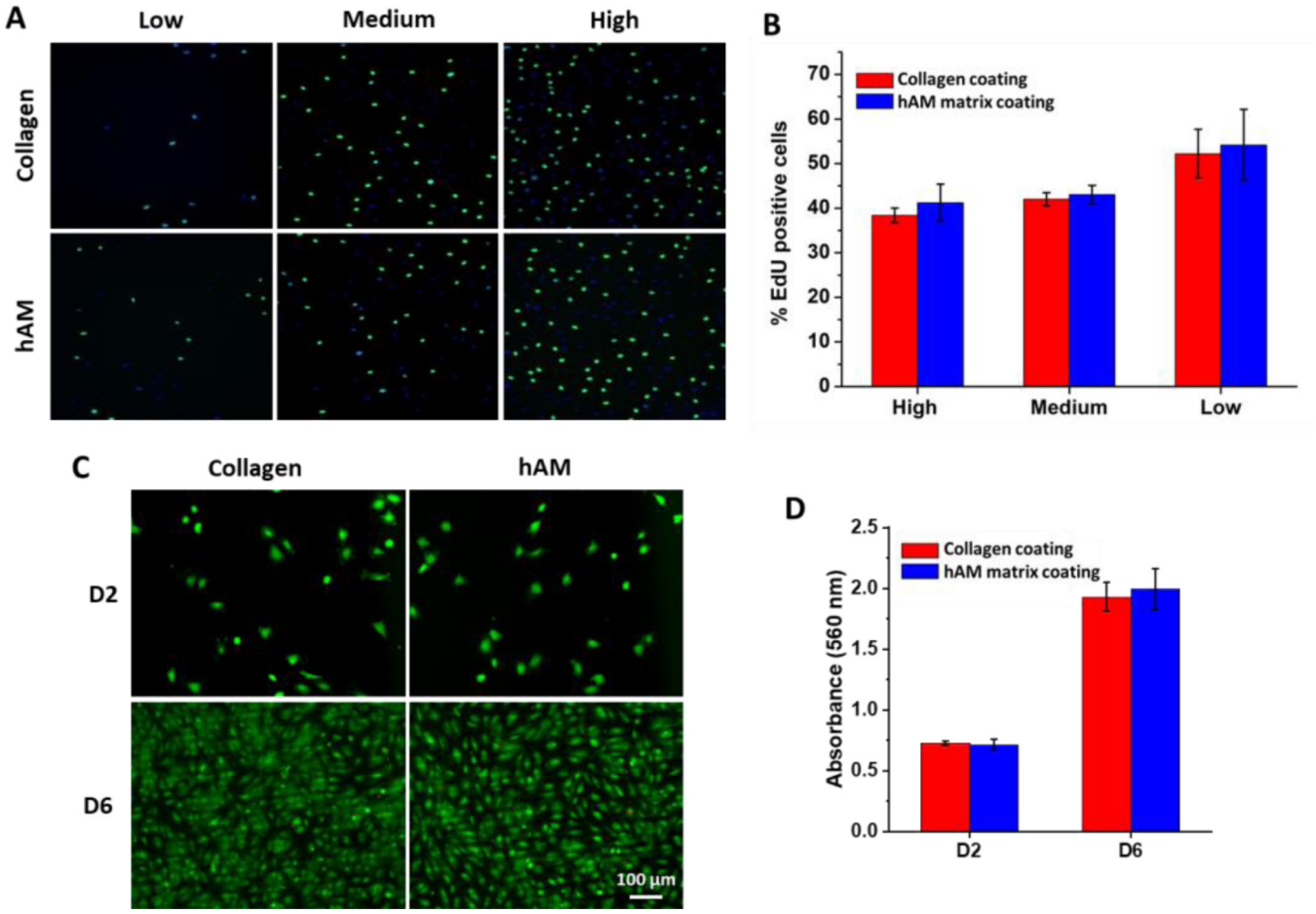

Figure 3: Proliferation, biocompatibility, viability of bovine aortic endothelial cells on hAM matrix.

BAECs were seeded at low (1000 cells/cm^2), medium (5000 cells/cm^2), and high density (10,000 cells/cm^2) on either hAM matrix or collagen-1. Proliferation was measured using EdU **(A)** and is presented as the percentage of total DAPI stained cells expressing positive EdU staining **(B)**. **(C)** Live/dead staining of ECs at days 2 and 6. Cells were seeded at 5000 cells/cm^2. **(D)** Cell viability assay at days 2 and 6. Cells were seeded at 5000 cells/cm^2.

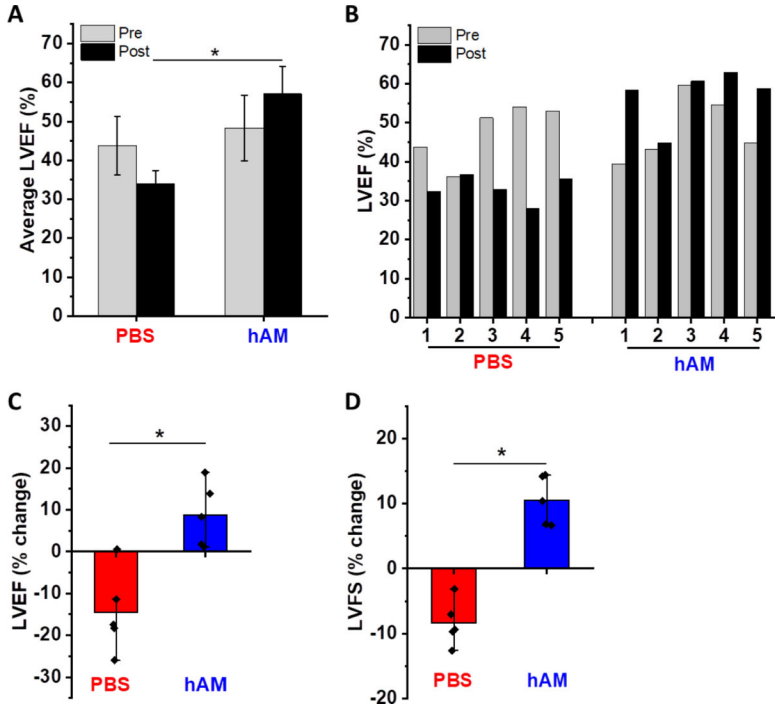

Figure 4: Effect of hAM matrix injection on LV ejection fraction (LVEF) and LV fractional shortening (LVFS) after 5 weeks following acute MI.

(A) Average LVEF before and after injection of PBS or hAM matrix, labeled as pre-treatment (Pre) or post-treatment (Post) respectively. **(B)** LVEF of each animal before and after injection of PBS or hAM matrix. **(C)** Average of LVEF changes by using pre-treatment value of each animal as a reference. **(D)** Average of LVFS changes by using pre-treatment value in each animal as a reference. n = 5 for each group, * $p < 0.05$.

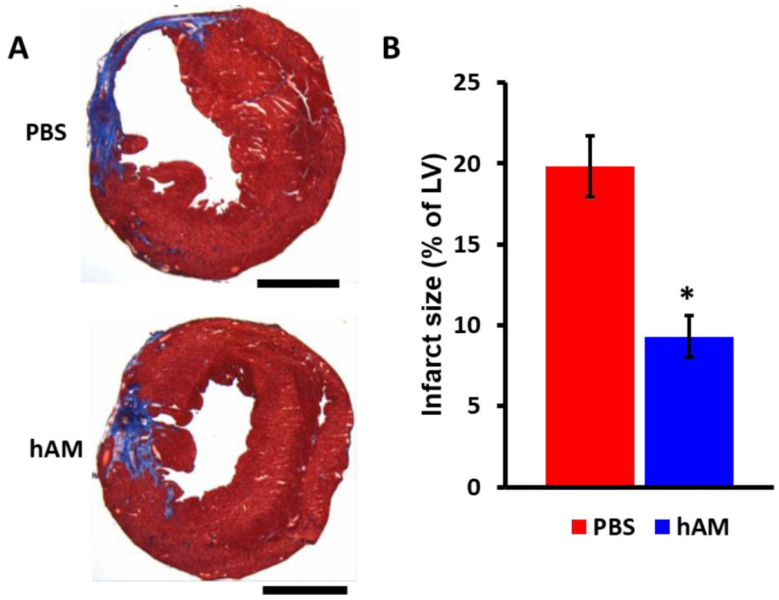

Figure 5. hAM matrix promotes adult cardiac regeneration after MI.

(A) Representative images of Masson trichrome-stained heart sections at 5 weeks after hAM matrix or PBS injection. Scale bars represent 4 mm. **(B)** Measurement of infarcted size at 5 weeks after hAM matrix or PBS injection analyzed by Masson trichrome staining. n = 5 for each group, * $p < 0.05$.